Received: 11 March 2017 | Accepted: 18 September 2017

DOI: 10.1111/1365-2745.12878

RESEARCH ARTICLE

Journal of Ecology | BRITISH ECOLOGICAL SOCIETY

Quantifying antecedent climatic drivers of tree growth in the Southwestern US

Drew M. P. Peltier[1,2] | **Jarrett J. Barber**[2] | **Kiona Ogle**[1,2]

[1]Department of Biological Sciences, Northern Arizona University, Flagstaff, AZ, USA

[2]School of Informatics, Computing, and Cyber Systems, Northern Arizona University, Flagstaff, AZ, USA

Correspondence
Drew M. P. Peltier
Email: dmp334@nau.edu

Funding information
Division of Biological Infrastructure, Grant/Award Number: 1458867

Handling Editor: Matt McGlone

Abstract

1. Variation in antecedent (past) climate conditions is likely to govern tree growth over long periods of time. Antecedent conditions are rarely considered in models of tree growth, representing a weakness in quantitative understanding of forest responses to climate variations.
2. We applied the stochastic antecedent modelling (SAM) framework to 367 International Tree Ring Data Bank chronologies in the southwestern US ("Southwest") representing eight conifer species. To better understand climatic and physiologic controls on tree growth, we quantify the effects of antecedent precipitation, temperature and Palmer Drought Severity Index (PDSI) over 60 months preceding and including the year of ring formation.
3. In *Pinus edulis*, *Pinus ponderosa* and *Pseudotsuga menziesii*, growth responded primarily to recent precipitation and temperature conditions (43%–49% of the response was driven by conditions during the year of ring formation), but to less recent PDSI conditions (>50% of response driven by conditions 13–48 months prior to the year of ring formation), though PDSI significantly affected growth at only 21% of sites. Combining extensive tree-ring data with monthly resolution climate data also reveals key climatic events, such as the effect of monsoon arrival date on growth, especially in *P. menziesii*, highlighting the ability of the SAM framework to identify climate effects at multiple time-scales.
4. Sensitivity to antecedent climate, baseline growth at average climate conditions and the strength of first order autocorrelation varied spatially, suggesting variation in mean growing conditions, non-structural carbohydrate storage, and/or seasonal precipitation contribution of the North American Monsoon may drive differences in growth sensitivities across species' ranges.
5. *Synthesis*. Our findings provide further evidence for multi-year legacy effects of climate conditions, particularly drought metrics, on tree growth. Antecedent climate and especially drought are key drivers of growth in these species, and associated climatic sensitivities and growth indices vary spatially. We argue such factors should be considered in modelling efforts. The spatial variability in antecedent climate sensitivities points to key differences in how different populations within a species range may respond to climate change, particularly if timing of weather events, such as monsoon arrival date, or annual precipitation amounts undergoes significant changes.

KEYWORDS
ecological memory, ecophysiology, legacy effects, non-structural carbohydrates, *Pinus edulis*, *Pinus ponderosa*, *Pseudotsuga menziesii*, tree–growth–climate interactions

1 | INTRODUCTION

Trees are long-lived organisms, integrating climate and physiological conditions over long periods to produce biomass at the expense of competing physiological processes such as reproduction, respiration and defence (Fritts, 1976). While antecedent (past) conditions are critical determinants of tree growth (Ogle et al., 2015; Peltier, Fell, & Ogle, 2016), particularly under stressful conditions (Jenkins & Pallardy, 1995; Stahle, Cleaveland, & Hehr, 1985; Tainter, Retzlaff, Starkey, & Oak, 1990), explicit accounting of antecedent climate and physiological states in growth models is rare. When antecedent climate is considered, approaches to selection vary widely (Bond-Lamberty et al., 2014; Tingley et al., 2012). Here, we apply a new modelling approach (Ogle et al., 2015), recently applied to diverse ecological processes (Barron-Gafford et al., 2014; Cable et al., 2013; Dal Bello, Rindi, & Benedetti-Cecchi, 2017; Ryan et al., 2015, 2017), to address these issues by directly determining temporal lags between tree growth and its exogenous (e.g. climatic) drivers across the southwestern US ("Southwest").

Dendrochronologists have gathered large amounts of tree-ring data, which can be used to evaluate factors driving tree growth. Site selection to avoid ecological influences such as competition, pests, and fire, and sampling near range limits or harsh microenvironments is key to avoiding "complacent" trees (Douglass, 1937), though mesic microhabitats may also contain strong climate signals (Carrer, Motta, & Nola, 2012). Potential influences of such factors are typically "removed" by detrending techniques to create standardized ring-width indices, subsequently averaged across trees to produce a stand-level chronology (Fritts & Swetnam, 1989). Chronologies are often used to understand correlations between tree or stand annual growth and specific past climate variables, such as monthly maximum temperatures in the summer preceding each growth period (e.g. Di Filippo et al., 2007). While orthogonal multiple regression approaches are commonly employed ("response functions," Blasing, Solomon, & Duvick, 1986; Fritts, 1962), monthly correlations are still sometimes independently estimated (e.g. Grace & Norton, 1990; Kirdyanov, Vaganov, & Hughes, 2007). Lagged correlations between growth and previous year's winter precipitation, summer maximum temperature, or summer precipitation are common, yet correlations with "older" climate variables are rarely studied (but see Bond-Lamberty et al., 2014; Johnson & Risser, 1973; Wilmking, Juday, Barber, & Zald, 2004).

There is mounting evidence that tree growth responds to climatic conditions occurring more than 1 year before the onset of growth, particularly in the context of changing climate. Application of a novel statistical model to raw tree-ring widths for *Pinus edulis* in southeastern Colorado, USA found that precipitation conditions experienced 2 years prior to the growth year influenced growth (Ogle et al., 2015). There is some evidence of effects of climate 3 years prior to ring formation (Mäkinen et al., 2002; Mazza & Manetti, 2013) and in rare cases, significant correlations between growth and climate occurring up to 6 years prior to ring formation have also been found (Becker, 1989; Peltier et al., 2016; Sarris, Christodoulakis, & Koerner, 2007). Another class of studies relates tree mortality to drought events occurring ten or more years ago (e.g. Bigler, Gavin, Gunning, & Veblen, 2007), while recent large-scale syntheses point to lags or legacy effects of drought on tree growth on the order of about 2–4 years in the Southwest (Peltier et al., 2016) and world-wide (Anderegg et al., 2015).

To address these limitations, we leveraged the large quantity of available tree-ring chronologies to gain a more complete understanding of how antecedent climate controls stand-level tree growth. Using data obtained from the International Tree Ring Data Bank (ITRDB), we implement the recently developed stochastic antecedent modelling (SAM) framework (Ogle et al., 2015) to address the following questions: (1) how do monthly precipitation, temperature, and drought stress experienced up to 4 years prior to ring formation influence tree growth? (2) How do the time-scales of influence (including time-lags) of these climatic variables vary among multiple dominant tree species? and (3) how do these antecedent effects (sensitivities and time-lags) vary spatially across the Southwest? Simultaneous estimation of the effects of key antecedent climate variables, their interactive effects, and their time-scales of influence is accomplished by applying the SAM framework to century-long annual tree-ring chronologies and monthly climate time-series data. Such analyses have the potential to greatly improve our understanding of the lagged and interacting factors controlling tree growth in this region.

2 | MATERIALS AND METHODS

2.1 | Data sources, selection and processing

All available chronologies from Arizona, Utah, Colorado and New Mexico were downloaded from the ITRDB portal via R (R Core Team, 2016) during September 2015. Chronology files were imported into R using the dplr package (Bunn, 2008). Chronologies were truncated at 1905 (used data for 1906 onward) to match availability of historic monthly climate data: total precipitation, mean temperature and self-calibrating Palmer drought severity index (hereafter, PDSI). We chose the self-calibrating index over the classical formulation because it is more comparable across regions (Dai, Trenberth, & Qian, 2004), easily available, widely used and straightforward to understand. The PDSI (2.5° resolution) data were obtained from NOAA (Dai et al., 2004). Monthly precipitation and temperature data were obtained from the Climatic Research Unit TS3.10 dataset, a gridded (0.5°) climate product (Harris, Jones, Osborn, & Lister, 2014).

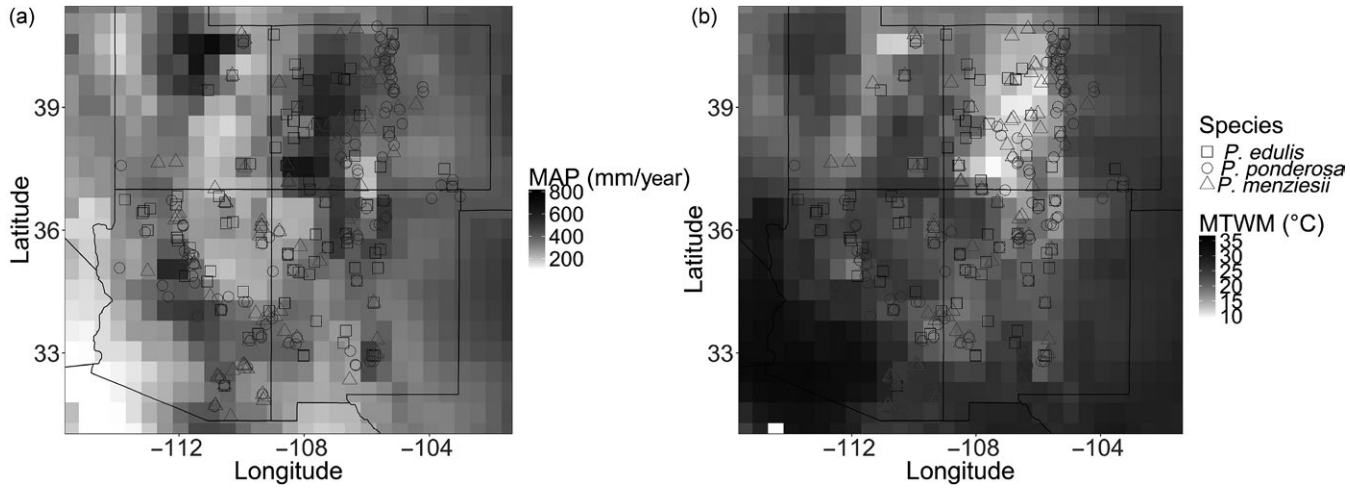

FIGURE 1 Chronology locations of the three best-represented species (PIED, *Pinus edulis*, squares; PIPO, *Pinus ponderosa*, diamonds; and PSME, *Pseudotsuga menziesii*, triangles), overlaid on the spatial variability (0.5° resolution) in (a) mean annual precipitation (MAP, mm/year) and (b) maximum temperature of the warmest month (MTWM, °C)

After preliminary analyses, we reduced the number of species to the eight best-represented species in our ITRDB dataset (367 chronologies, all conifers, total N = 28,530 annual growth indices representing more than 10,000 trees): *Picea engelmannii* Parry Ex. Engelm. (PCEN; Engelmann spruce), *Pinus aristata* Engelm. (PIAR; bristlecone pine), *Pinus contorta* Dougl. Ex. Loud. (PICO; lodgepole pine), *P. edulis* Engelm. (PIED; pinyon pine), *Pinus flexilis* James (PIFL; limber pine), *Pinus ponderosa* Dougl. Ex. Laws. (PIPO; ponderosa pine), *Pinus strobiformis* Engelm. (PIST; Southwestern white pine) and *Pseudotsuga menziesii* (Mirb.) Franco (PSME; Douglas fir). Three species (*P. ponderosa*, *P. edulis* and *P. menziesii*) constituted 87.5% of this dataset (Figure 1).

We note that the ITRDB chronologies were produced by a variety of detrending techniques, which we do not account for because this information is not universally available in the ITRDB. While detrending choices made in producing these chronologies may alter the strength of the signals we detect, use of tree-ring chronologies to make inference about lagged responses has precedence (Anderegg et al., 2015). Working with raw ring-width data and incorporating an age-detrending model at the core level would seem like a potentially powerful and more appropriate method for detecting lagged effects of climate (Peltier et al., 2016). However, combining this type of approach with the computationally demanding SAM framework is computationally impractical at this time. Thus, to explore tree–growth–climate relationships at a regional scale using the SAM approach, we have elected to use stand-level, detrended chronologies.

2.2 | Model description

The principles and motivation underlying the SAM framework have been described elsewhere (Ogle et al., 2015; also see Ogle & Barber, 2016 for additional examples), including a simple application to tree-ring widths representing 10 trees of a single species at one site. Here, we extend the SAM framework to include different sites (chronologies) and species. We refer to the annual tree-ring chronology indices as "growth." The definition of antecedent variables and their effects on the response (i.e. annual tree growth) constitute the key concept of the SAM model. An antecedent variable is defined as a weighted average of past observed values. These antecedent variables are used as covariates in the regression of tree growth on climate, each having its own effect parameter as in classical linear regression.

To illustrate, let $P^{\text{ant}}_{y,c}$ denotes antecedent precipitation, constructed for year y and site (or chronology) c; chronology is analogous to a unique species-site combination, and only one species occurs at each site. Thus, for simplicity we refer to chronologies as sites. Let $P_{y\text{-}t,m,c}$ denotes monthly precipitation associated with site c for month m (m = 1, 2, …, 12 for January, February, …, December) and for t years into the past (t = 0, 1, …, 4 for current year, last year, …, 4 years prior) relative to year y. This 5-year period follows (Ogle et al., 2015) and is comparable to the maximum recovery time following drought (Anderegg et al., 2015; Peltier et al., 2016), though longer lags could be considered. Further, let $w_{t,m,s,v}$ denotes the antecedent importance weight, estimated for year t into the past, month m, species s (s = 1, 2, …, 8), and variable v (e.g. v = 1 for precipitation). Then,

$$P^{\text{ant}}_{y,c} = \sum_{t=0}^{4} \sum_{m=1}^{12} w_{t,m,s(c),1} \cdot P_{y-t,m,c} \quad (1)$$

where $s(c)$ indicates the species s associated with site c. Antecedent temperature (T^{ant}) and drought (D^{ant}) are constructed identically, each with their own unique species-specific weights ($w_{t,m,s,2}$ and $w_{t,m,s,3}$, respectively). Precipitation, temperature and drought conditions occurring after the cessation of growth cannot effect ring width during the same year, thus weights for October, November and December (m = 10, 11, 12) of the current year (t = 0) are fixed at zero for all three climate variables. While growth cessation date may vary across sites or years, most species in this region cease forming rings in September (Adams & Kolb, 2005; Barger & Woodhouse, 2015; Fritts, Smith, Cardis, & Budelsky, 1965).

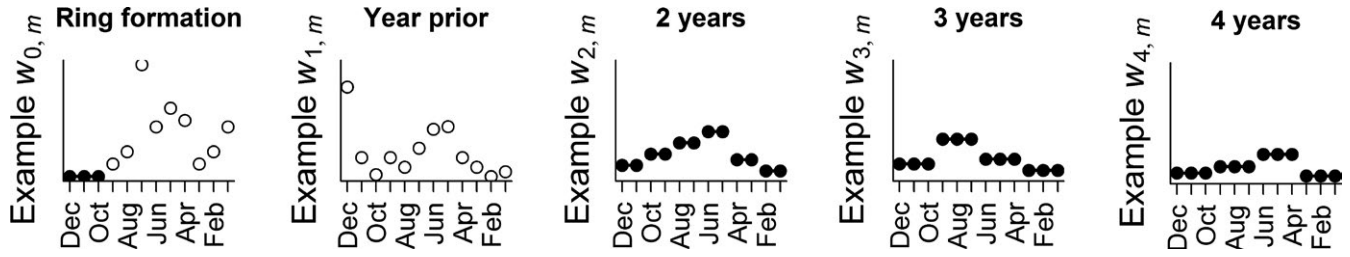

FIGURE 2 Example patterns of the 60 monthly weights ($w_{t,m}$). Following our assumption of declining resolution with greater time into the past, weights that are constrained to be equal to neighbouring weights are denoted by filled circles linked by lines. Unfilled circles represent unconstrained weights that can differ from neighbouring weights. The monthly weights for October, November and December of the year of ring formation are constrained to be exactly 0, as these represent time periods that are expected to occur after the average cessation of the growing season. All other weights are treated as unknown and estimated as part of the stochastic antecedent modelling (SAM) framework

We extend the weights to some past time point (i.e. 4 years ago) to allow the data to inform the importance of past conditions, rather than imposing an ad hoc selection of only a single previous year's climate covariates (e.g. previous-July temperature or previous-April precipitation). Because we assume the ability of the model and data to resolve unique monthly weights declines with time into the past (Figure 2), we estimate individual monthly weights for only the most recent 2 years (t = 0 and 1). Further into the past, we only estimate six weights representing periods of 2 months for t = 2 (i.e. we assume $w_{2,1,s,v} = w_{2,2,s,v}$ and $w_{2,3,s,v} = w_{2,4,s,v}$), and for t = 3 and 4, we estimate four unique weights for each year t (assume $w_{t,1,s,v} = w_{t,2,s,v} = w_{t,3,s,v}$ and $w_{t,4,s,v} = w_{t,5,s,v} = w_{t,6,s,v}$, etc.). Thus, while each species' set of weights has 60 components, there are only 35 "free" weight parameters estimated for each species; the remaining 25 weights are either fixed at zero (post ring formation in t = 0) or set equal to one of the 35 free weight parameters (see Figure 2). Monthly weights are constrained to sum to one across all t and m for each species s and variable v. We also compute annual weights $W_{t,s,v}$ for each calendar year t into the past by summing the month weights (ws) over all months m. While we considered the use of more ecologically meaningful "hydrologic years," any such delineation is inherently arbitrary, and would likely differ across species (or within a species' range). With the concept of antecedent variables established, we continue to specify the model.

The data model gives the likelihood of the observed growth G, where we define G = log(RWI + 1), where RWI is the site ring-width index obtained from the ITRDB chronology files. We assume a normal distribution for G, with mean μ and variance σ^2. The data and expected (mean) log-scale RWI vary at the level of year y and site c:

$$G_{y,c} \sim \text{Normal}(\mu_{y,c}, \sigma^2) \tag{2}$$

Expected, log-scale growth (μ) is modelled as a function of the antecedent climate covariates of precipitation (P^{ant}), temperature (T^{ant}) and PDSI (D^{ant}) at each site (c), along with an intercept and 1st-order autoregressive term for each site. Based on preliminary analyses, we also found it useful to include the $P^{\text{ant}} \times D^{\text{ant}}$ and $T^{\text{ant}} \times D^{\text{ant}}$ two-way interactions; we did not include a $P^{\text{ant}} \times T^{\text{ant}}$ interaction as D^{ant} represents a nonlinear interaction between precipitation and temperature. On the original RWI scale, a typical 1st-order autoregressive model assumes $\text{RWI}_y = \alpha\text{RWI}_{y\text{-}1}$; on the transformed scale, this implies $G_y = \log(\alpha\text{RWI}_{y\text{-}1} + 1)$. The log-scale model also implies multiplicative effects of the covariates on the raw scale (i.e. for RWI), an approach that worked well in a previous application of SAM to tree-ring data (Ogle et al., 2015). We assume climate and the autoregressive process simultaneously affect growth, and the effects of these predictor variables are denoted by α; we allow for each α to vary by site c such that:

$$\begin{aligned}\mu_{y,c} = {} & \alpha_{c,1} + \alpha_{c,2} P^{\text{ant}}_{y,c} + \alpha_{c,3} T^{\text{ant}}_{y,c} + \alpha_{c,4} D^{\text{ant}}_{y,c} \\ & + \alpha_{c,5} P^{\text{ant}}_{y,c} D^{\text{ant}}_{y,c} + \alpha_{c,6} T^{\text{ant}}_{y,c} D^{\text{ant}}_{y,c} + \log(\alpha_{c,7} \text{RWI}_{y-1,c} + 1)\end{aligned} \tag{3}$$

Thus, conditional on the antecedent covariates, Equation (3) can be viewed as a linear regression with random coefficients $\alpha_{c,p}$ (for p = 1, 2, …, 7 parameters). However, the antecedent variables are not fixed covariates, as in a typical linear regression, and are functions of the unknown weights as in Equation (1). This results in a nonlinear regression when not conditioning on the antecedent variables.

2.3 | Prior specification

We implemented the model (Equations 1–3) in a hierarchical Bayesian framework. We assumed a hierarchical model (prior) for the site-level regression parameters (αs), which vary around species-level means, μ_α, with species-level variances, $\sigma_\alpha{}^2$, such that for parameter p:

$$\alpha_{c,p} \sim \text{Normal}(\mu_{\alpha_{s(c),p}}, \sigma^2_{\alpha_{s(c),p}}) \tag{4}$$

In the case of $\alpha_{7,c}$, the autoregressive effect, this prior was restricted to positive values (normal prior truncated at zero), as would be consistent for an AR(1) model.

Except for the autoregressive effects, the species-level parameters were also modelled hierarchically with global means (M_{α_p}) and variances ($S^2_{\alpha_p}$) such that for species s and parameter p ($p \neq 7$):

$$\mu_{\alpha_{p,s}} \sim \text{Normal}(M_{\alpha_p}, S^2_{\alpha_p}) \tag{5}$$

This hierarchical prior allowed us to obtain more precise parameter estimates for species associated with comparably few chronologies. Global parameters, M_{α_p} and S_{α_p} (standard deviations), were given

diffuse Normal(0, 10,000) and Uniform(0, 100) priors, respectively. The species-level autoregressive parameter ($\mu_{\alpha_{s,7}}$) and standard deviations ($\sigma_{\alpha_{s,p}}$) were assigned independent Uniform(0,100) priors.

We note that all climate covariates are centred on their site-level mean values (averaged across all years). Thus, we can compute indices of baseline growth (G^*) at average climate conditions at both the site- and species-level such that:

$$G_x^* = A_{x,1} + \log\left(A_{x,7}\overline{\mathrm{RWI}}_s + 1\right) \text{ and } \mathrm{RWI}_x^* = \exp\left(G_x^*\right) - 1 \quad (6)$$

where G^* is the log-scale and RWI* is the ring-width index-scale baseline growth term, respectively; $x = c$ for site (with $A = \alpha$) or s for species (with $A = \mu_\alpha$). $\overline{\mathrm{RWI}}_s$ is the average ring-width index for species s, averaged across all years and chronologies considered in this study.

In addition to estimating the "overall" effects (αs and μ_αs) and the baseline growth terms (G^* and RWI*), we also estimate the weight parameters (ws [monthly] and Ws [annual]). Loosely, we might view the effects as indicating the growth sensitivity to antecedent conditions and the weights as the temporal pattern of the antecedent effects. So that antecedent weights sum to 1 across years t and months m for each covariate (P^{ant}, T^{ant} and D^{ant}) and species s, we define $\mathbf{w}_{s,v}$ to be the vector of the 35 "free" weights for each species s and variable v, and give $\mathbf{w}_{s,v}$ a vague Dirichlet prior:

$$w_{s,v} \sim \mathrm{Dirichlet}(1,1,\ldots,1) \quad (7)$$

This prior results in the prior expectation that all 35 weights are the same.

2.4 | Implementation

The model was implemented in JAGS 4.0.0 (Plummer, 2003) via the package rjags (Plummer, 2013) in R (R Core Team, 2016) using supercomputing resources at Northern Arizona University (https://nau.edu/hpc). Three parallel MCMC chains were used to sample from the posterior parameter space and assessed for convergence. All iterations during the burn-in phase (pre-convergence) were discarded and the model was updated again to obtain ≥3,000 relatively independent samples after thinning.

2.5 | Posterior analyses

Posterior distributions for each parameter are summarized by the posterior mean, standard deviation, and 95% central credible interval (CI) defined by the 2.5th and 97.5th percentiles of the marginal posterior distributions. To explore spatial patterns in baseline growth (RWI_c^*), antecedent climate and endogenous autoregressive effects (αs), we conducted classical linear regressions of site- (i.e. chronology-) level parameters (posterior means for each $\alpha_{c,p}$ and RWI_c^*) on centred latitude, longitude and their interaction (degrees), for each of the three best-represented species (*P. menziesii*, *P. ponderosa* and *P. edulis*) using the base R (R Core Team, 2016) lm function.

3 | RESULTS

3.1 | Model fit

A regression of predicted vs. observed G data yielded $R^2 = 0.59$, which we may expect to improve with higher resolution climate data (here, 0.5° for precipitation and temperature; 2.5° for PDSI). The model showed slight bias (slope of predicted vs. observed = 1.04), with slight overestimation of growth at low RWI and slight underestimation at high RWI. Species-specific R^2 values were roughly similar for most species (R^2 = 0.56–0.61), but were as low as R^2 = 0.48 (PIAR, PICO) and as high as R^2 = 0.80 (PCEN; Figure S1). Regression of predicted vs. observed G data for each site gave the highest R^2s in the southwestern portion of the region and lowest in the northeastern portion (Figure S2).

3.2 | Parameter estimates

Posterior means, standard deviations and 95% CIs for all model parameters are reported in Tables S1–S3 and Figure S3, including the site-, species- and global-level means and standard deviations. Here, we focus on site-level baseline growth indices, autoregressive terms, antecedent climate effects and antecedent importance weights.

3.3 | Site-level effects

Site-(or chronology-) level baseline growth (RWI_c^*) was significantly greater than zero across all sites, with an average posterior mean of 1.076 (Figure 3a). However, RWI_c^* varied about 5-fold across sites, from 0.278 ± 0.084 (posterior mean; a PSME site) to 1.456 ± 0.060 (a PIED site). Most (84%) of the site-level P^{ant} effects (α_2) were significantly positive (Figure 3b), 73% of the T^{ant} effects (α_3) were significantly negative (Figure 3c), and 21% of the D^{ant} effects (α_4) were significantly positive except for two eastern PIED sites (Figure 3d). Only 8% of the $P^{\mathrm{ant}} \times D^{\mathrm{ant}}$ effects (α_5) were significantly negative, and only for a subset of PIED and PIPO sites (Figure 3e). There were no significant site-level $T^{\mathrm{ant}} \times D^{\mathrm{ant}}$ effects (α_6; thus, results not shown). Depending on species and site, the autoregressive term (α_7) varied from relatively strong (some PCEN sites; e.g. α_7 = 0.522 [0.412, 0.645]) to extremely weak (some PIPO sites; e.g. α_7 = 0.0003 [0.000006, 0.0012]) (Figure 3f); the prior for α_7 eliminated the possibility of α_7 being exactly zero.

3.4 | Spatial patterns in site-level effects

For the three best-represented species (PIED, PIPO and PSME), linear regressions of each of the site-level effects against latitude, longitude and their interaction revealed strong spatial patterns in baseline growth, the autoregressive parameters and the effects of antecedent climate variables across the Southwest (Table 1, Figure S4). We highlight significant regressions that explained >10% of the spatial variation in the site-level effects. Baseline growth decreased from east to west (PIED: R^2 = 0.47; PIPO: R^2 = 0.29; PSME: R^2 = 0.19). For PIPO, baseline growth was also lower for northern sites, although there was a positive latitude

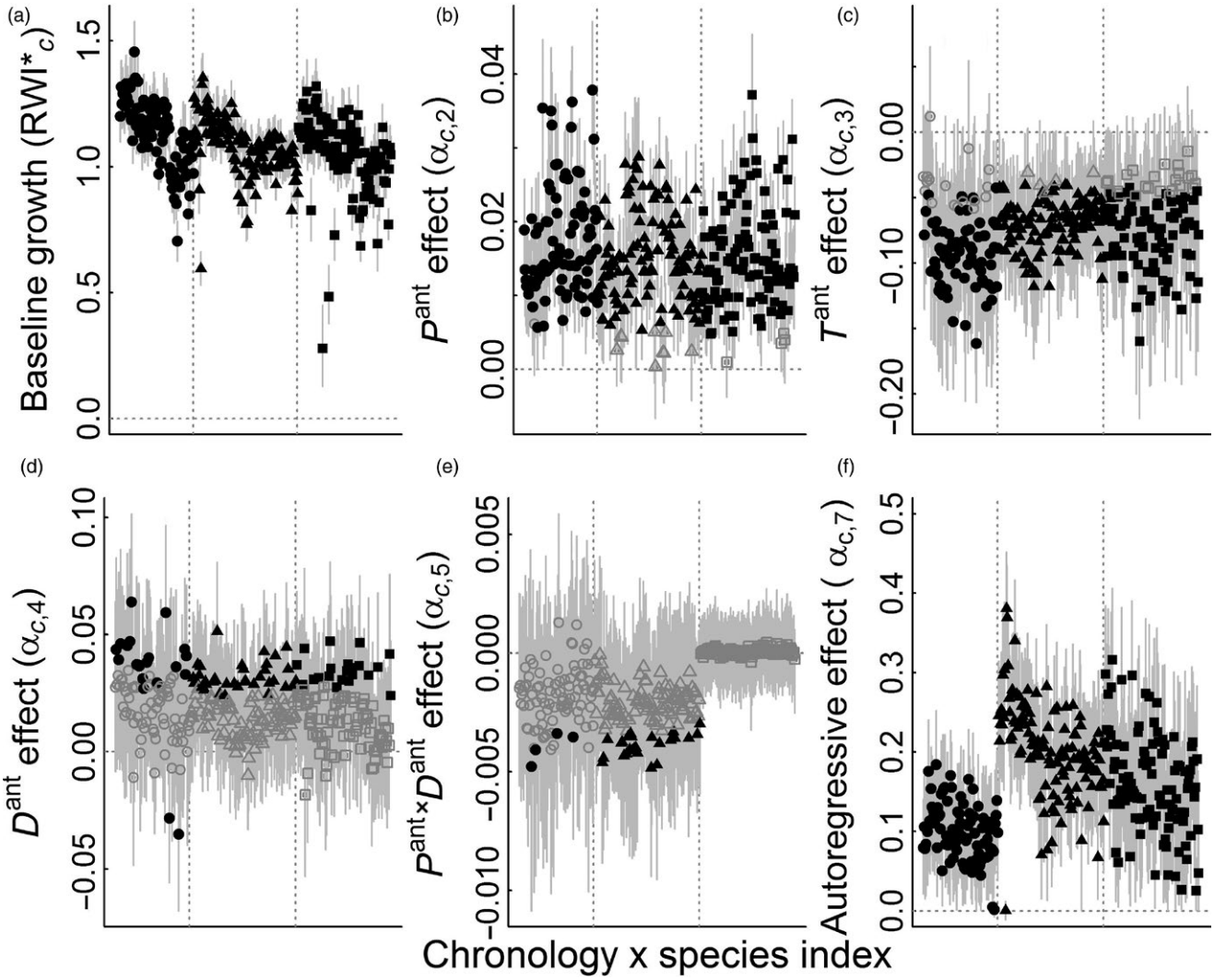

FIGURE 3 Posterior means (symbols) and 95% Bayesian credible intervals (CIs, grey whiskers) for the chronology- (site-) level parameters, including: (a) RWI_c^* (baseline growth); the effects of antecedent (b) precipitation (P^{ant}), (c) temperature (T^{ant}), and (d) drought (D^{ant}); the (e) $P^{ant} \times D^{ant}$ interaction; and the (f) 1st order autoregressive effect. Within each plot, effects are grouped by species, with species separated by vertical dotted lines (only the three best represented species are included here, in order left to right: *Pinus edulis* (PIED), circles; *Pinus ponderosa* (PIPO), triangles; *Pseudotsuga menziesii* (PSME), squares; see Table S1 for other species). Within each species, effects are sorted by longitude of the site, from west (left) to east (right). Effects with CIs that do not overlap zero (signified by black, filled symbols) are considered significant at $p < .05$ (open symbols indicate non-significant effects). The $T^{ant} \times D^{ant}$ interaction term is omitted as none were significant

by longitude interaction. The magnitude of the autoregressive effect strength decreased towards the northeastern portion of the region for PIPO ($R^2 = 0.26$) and towards the east for PSME ($R^2 = 0.22$). The effect of P^{ant} also decreased towards the northwest for PIED ($R^2 = 0.17$), and the effect of D^{ant} decreased towards the east for PIED ($R^2 = 0.12$).

3.5 | Antecedent importance weights

For species where the effects of antecedent climate were not significant (PIAR, PICO and PCEN), the antecedent weights (*w*s in Equation 1) are not meaningful, so we only report results for the five species with significant antecedent climate responses (i.e. PIED, PIFL, PIPO, PIST and PSME; see Figure 4). Pairwise correlations (Pearson's *r*) of the monthly weights split these species into two groups characterized by similar weights: first, PIED, PIPO and PSME ($r = .73–.83$) and second, PIST and PIFL (both white pines, $r = .84$, Figure S5). We emphasize that the weights (*w*s [monthly] and *W*s [annual]) describe the temporal pattern of the antecedent effects, while the coefficients (αs [site-level] and μ_αs [species-level]) describe both the strength (via the magnitude and significance level) and direction (i.e. the sign) of the antecedent effects. For example, while all weights are positive (irrespective of the climate variable), the effects of temperature were negative, and so weights associated with the T^{ant} term describe the temporal pattern of that (negative) response.

Precipitation and temperature importance weights are strongly concentrated in the year of and the year prior to ring formation. The largest *w*s for P^{ant} occur in the current growing season and fall and

TABLE 1 Summary of the linear regressions of chronology-(site-) level effects (posterior means of each parameter) against latitude (Lat), longitude (Lon), and their interaction (Lat × Lon) for the three best-represented species in the dataset (see Figure 1 for description of species). Climate covariates were centred around site-level means. Model fit statistics include the adjusted R^2 for the overall model and individual significance levels for effects: ***p < .001, **p < .01, *p < .05 and $^{\dagger}p$ < .1. The sign (+ or −) of each covariate (Lat, Lon, Lat × Lon) is indicated for each regression. RWI_c^* is baseline growth at average climate conditions

	PIED				PIPO				PSME			
Parameter	Lat	Lon	Lat × Lon	R^2	Lat	Lon	Lat×Lon	R^2	Lat	Lon	Lat×Lon	R^2
RWI_c^*		−***		0.47	−***	−***	+*	0.29		−***		0.19
α_7 (AR1)		−**		0.07	−***	−***		0.26		−***		0.22
α_2 (P^{ant})	−***	+**		0.17					−†	+*		0.07
α_3 (T^{ant})		−*		0.04	+*			0.04	+†			0.04
α_4 (D^{ant})		−***		0.12		−*		0.01		−**		0.07
α_5 ($P^{ant} \times D^{ant}$)					+**	−*		0.07			+*	0.06

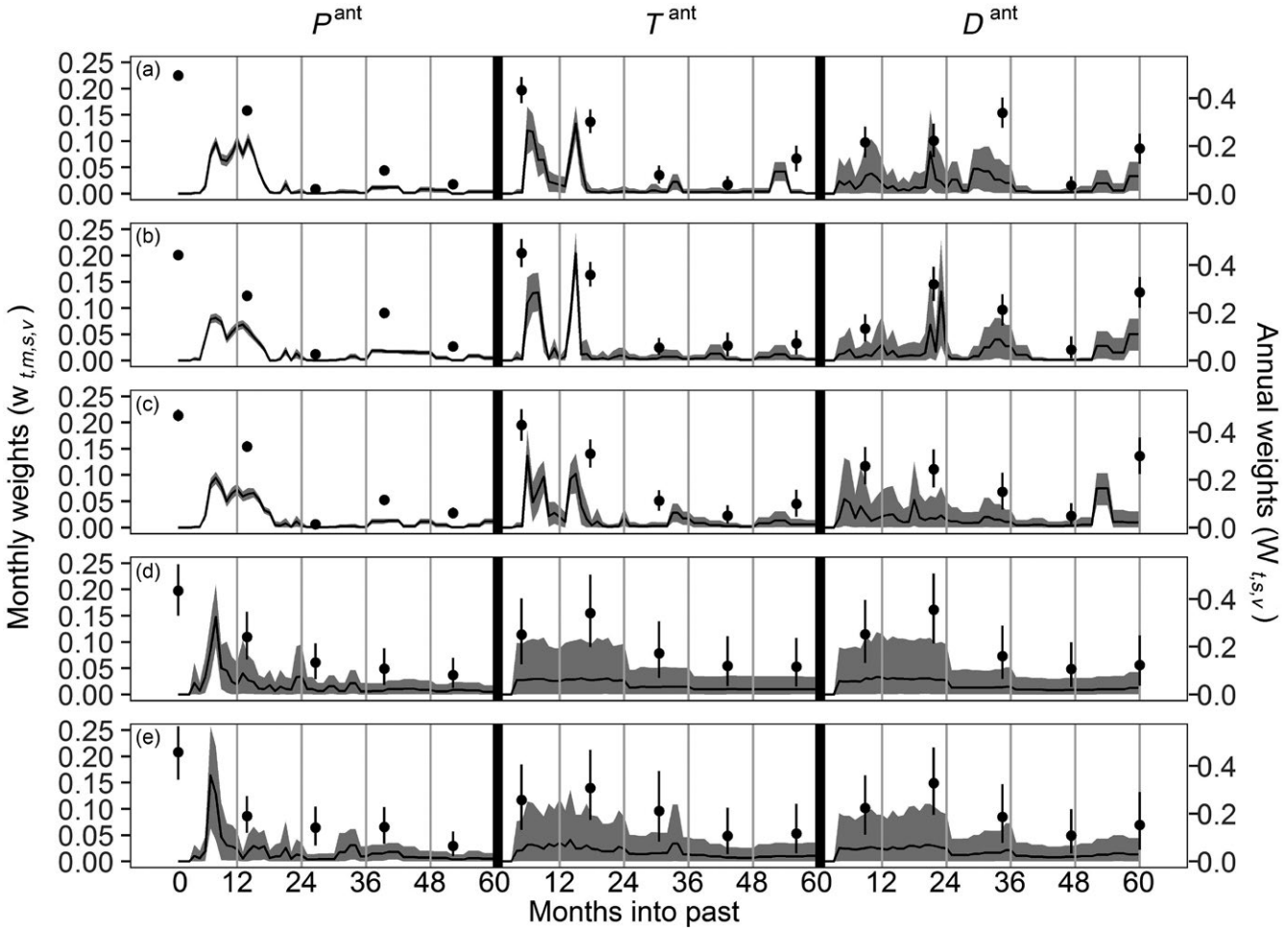

FIGURE 4 Monthly antecedent weights ($w_{t,m,s,v}$) and yearly weights ($W_{t,s,v}$) for each of the three antecedent climate variables for five species (rows): (a) *Pinus edulis* (PIED), (b) *Pinus ponderosa* (PIPO), (c) *Pseudotsuga menziesii* (PSME), (d) *Pinus flexilis* (PIFL) and (e) *Pinus strobiformis* (PIST). Columns correspond to the antecedent climate variables, which are separated by vertical black lines (from left to right: P^{ant}, T^{ant} and D^{ant}; see Figure 1 for definitions). Within each antecedent variable (single panel), vertical grey lines separate years (left: year of ring formation, right: 4 years prior to ring formation). Months are indicated on the x-axes (from left: December of year of ring formation, right: January of 4 years prior to ring formation). Black lines are the posterior means of monthly weights ($w_{t,m,s,v}$), with the grey shaded area representing the 95% Bayesian credible intervals (CIs). Filled circles are the posterior means of yearly weights ($W_{t,s,v}$; sum of monthly weights within a given year-antecedent variable) and whiskers are the 95% CIs. Weights are constrained to sum to 1 within each climate variable and species. October–December of current year weights (months 1–3) are a priori set equal to zero

winter preceding ring formation (e.g. June of current year for PIST, Figure 4e). The largest *w*s for T^{ant} occur during the middle to late current growing season and previous fall (e.g. October of previous year for PIPO, Figure 4c). While large *w*s are mostly grouped into seasons, species may also respond uniquely to conditions in individual months. So while PIPO growth is driven by temperature conditions throughout late spring and early summer in the year of ring formation (Figure 4b), PSME responds most strongly to July temperature during the same year (Figure 4c). Finally, the monthly *w*s associated with D^{ant} are less distinguishable than those associated with P^{ant} or T^{ant} (Figure 4, rightmost column), but indicate a tendency for conditions further into the past (beyond last year) to be important.

Importantly, climate conditions occurring 2–4 years prior to ring formation, particularly for D^{ant}, also drive growth. For both PSME (Figure 4c) and PIPO (Figure 4b), PDSI conditions experienced 4 years prior to growth were important predictors of growth (July–September for PSME and January-March for PIPO). Yearly weights (*W*s) more clearly show the importance of PDSI 4 years prior to ring formation for growth in PSME (*W* not significantly different from current or prior year's *W*s, Figure 4c), as well as the importance of PDSI 2 years prior to ring formation for PIED (highest *W*, Figure 4a; $p < .05$). Summing groups of yearly weights (*W*s) shows PDSI conditions 2–4 years prior to ring formation account for 50%–56% of the D^{ant} importance weights in PIPO, PIED and PSME, while a single year (the year of ring formation) accounts for nearly half (43%–49%) of the P^{ant} and T^{ant} importance weights (Figure 4a–c). The two white pines (PIFL and PIST, Figure 4d,e) show similar patterns with respect to P^{ant} (the year of ring formation accounts for 43%–46% of the total P^{ant} importance weight) and D^{ant} (2–4 years prior to ring formation accounts for 40%–45% of total D^{ant} importance weight), but not T^{ant} (the year of ring formation accounts for only 25%–26% of the total T^{ant} importance weight).

4 | DISCUSSION

To improve understanding of the dependence of tree growth on antecedent climate, we applied the SAM framework (Ogle et al., 2015) to stand-level tree-ring chronologies spanning 100 years representing eight conifer tree species at 367 sites across the Southwest. The model simultaneously evaluates the effects of precipitation, temperature and drought (PDSI) during and up to 4 years prior to the year of ring formation, along with the relative importance ("weights") of monthly climate in each antecedent time period. Across species, climate conditions experienced during the year of and the year prior to ring formation were often the most important (highest importance weights), which is generally consistent with many tree-ring studies that evaluate correlations between annual ring widths or ring-width indices and monthly climate variables (Bond-Lamberty et al., 2014; Carrer & Urbinati, 2006; Chen, Welsh, & Hamann, 2010; and see Appendix S1). Importantly, however, we found that integrated measures of drought occurring up to 4 years prior to ring formation are also important predictors of growth (i.e. PDSI occurring 4 years prior to growth accounted for *c*. 15%–30% of the importance weight in *P. menziesii*, *P. edulis* and *P. ponderosa* [PSME, PIED and PIPO]; Figure 4a–c). We also document significant spatial variation in growth parameters within species, with baseline growth rates, 1st order autocorrelation, and sensitivity to antecedent climate varying along latitudinal or longitudinal gradients. We discuss potential mechanisms and implications of these results for understanding physiological mechanisms of climate legacies and for developing tree growth models that account for such effects.

4.1 | Physiology of tree responses to climate

In general, parameter estimates agreed well with climate correlations from the dendrochronology literature, with clear physiological interpretations. Positive correlations with winter precipitation received immediately prior to ring formation are often attributed to soil moisture recharge or snow pack effects, resulting in greater growing season moisture availability (Campelo et al., 2009). Negative correlations between ring width and previous and current growing season temperature in multiple *Pinus* species are well-documented in the Southwest, and have been attributed to increased drought stress or increased respiration rates (Adams & Kolb, 2005). Positive effects of PDSI (higher PDSI values indicate more favourable conditions) during the previous winter, current growing season and monsoon period indicate a positive growth response to high moisture availability during these periods, due to decreased water stress (Adams & Kolb, 2005; Copenheaver, Kyle, Stevens, & Kamp, 2005).

Application of the SAM framework also detected correlations with less clear interpretations, or that do not have much precedence in the dendrochronology literature, such as positive effects of late winter (*P. ponderosa*) or spring (*P. edulis*) previous-year PDSI. Cool and wet conditions (higher PDSI) in the early growing season may lead to decreased respiration during the early growing season, when trees are flushing new needle crops (and thus increased assimilation by the previous year's needle crops (Michelot, Simard, Rathgeber, Dufrêne, & Damesin, 2012). Similarly, negative P^{ant} by D^{ant} interaction terms indicate sensitivity to precipitation (P^{ant}) is lower during periods characterized by high D^{ant} (more favourable, less drought-like conditions), suggesting a saturating effect of precipitation such that additional precipitation does not increase tree growth when past conditions have been cool and wet. Finally, the importance of climate at monthly timescales suggests physiological responses to key climatic events: a strong negative response to July temperature in the year of ring formation for *P. menziesii* likely results from variability in the onset date of the North American Monsoon (NAM), which "breaks" the summer drought and decreases summer temperatures in the Southwest (Babst et al., 2016). Variation in this arrival date could have severe implications for growth in this species, particularly under anticipated increases in atmospheric moisture demand (Szejner et al., 2016).

4.2 | Importance of antecedent climate

Much of the dendrochronology literature is focused on ring width responses to current or recent climate—in our informal review of 200

peer-reviewed dendrochronology studies (Appendix S1), less than 5% of studies consider climate beyond about 1 year prior to ring formation—and these 2 years are the major focus of most dendrochronologists interested in reconstructing climate conditions (Douglass, 1937; Fritts, 1966, 1976; Fritts & Swetnam, 1989). We also find a majority of the strongest correlations of ring width with climate variables during and 1 year preceding the year of ring formation (Figure 4). However, we also provide strong evidence that *P. edulis*, *P. ponderosa* and *P. menziesii* are responding to conditions occurring 3–4 years prior to ring formation, and that (in the case of PDSI) correlations with antecedent conditions more than a year prior to ring formation are of similar or larger magnitude than those with growing season conditions (Figure 4c). While other studies have found lagged effects on growth of similar or longer length for the effects of multiple years of cumulative precipitation (Mazza & Manetti, 2013; Sarris et al., 2007), this finding of correlations between ring width and climate during discrete periods 4 years in the past for multiple species is somewhat novel (but see Becker, 1989). Less distinguishable and lower weights for recent PDSI conditions could be due to the integration of previous climate conditions inherent in the PDSI calculation (Dai et al., 2004). We note that while seasonal correlations are consistent with other studies (e.g. negative correlations with summer temperature, positive correlations with growing season precipitation), quantification at monthly resolution of growth–climate correlations shows that there is important month to month variation within a season across species (Figure 4). Furthermore, most studies do not investigate climate correlations during the early part (January–April) of the year prior to ring formation (Carrer & Urbinati, 2006; Chen et al., 2010; Villalba, Veblen, & Ogden, 1994), and fewer studies evaluate the lagged effects of PDSI, yet we found high correlations between ring-width indices and Jan.–Apr. PDSI of the year prior to ring formation for at least one widespread species (*P. ponderosa*).

We acknowledge that there are potential issues with applying the SAM approach to chronologies to infer the time-scales and lags associated with antecedent climate effects on tree growth, and that lags may actually be somewhat underestimated here. First, the chronologies were detrended by various methods, and it is likely that stronger effects of older climate would be found in applications to ring-width series detrended solely for age effects. In particular, chronologies created by spline-type detrending methods remove variation at multi-year time-scales such as that related to competition in forest interiors (Cook & Peters, 1981), and this may weaken correlations with older climate. Second, depending upon the information of interest for a given chronology, removal of variation at these time-scales may obscure signals from stochastic events such as extreme droughts (Anderegg et al., 2015; Peltier et al., 2016), release from competition (or growth inhibition) due to insect outbreaks or fire (Keen, 1937; Weaver, 1943), or strong El Niño events (Veblen, Kitzberger, & Donnegan, 2000) that would result in greater dependence of tree-ring width on events many years prior to ring formation. In support of this expectation, an earlier application of a SAM model to *P. edulis* raw ring widths found higher importance weights of less recent (e.g., 3–4 years prior to ring formation) precipitation and temperature variables (Ogle et al., 2015). Finally, we also caution that bias in site and tree selection typical of dendrochronologies (Nehrbass-Ahles et al., 2014) could lead to monthly weights and climatic sensitivities that may not accurately represent all trees within these species. So-called "complacent" trees (Douglass, 1937) could potentially respond somewhat differently to climate, but we are limited by the data available in the ITRDB.

4.3 | Mechanisms underlying lags in tree chronologies

The physiological mechanisms underlying short lags (1–2 years) in tree-ring records are fairly well studied. One classical explanation, particularly for conifers, is that trees retain needle crops for multiple years, and thus poor or above average needle production in response to climatic conditions may result in photosynthetic deficit or surplus for a number of subsequent years (Fritts, 1976). Trees can also store surplus non-structural carbohydrates (NSCs), and draw on these reserves for multiple years or in times of stress (Chapin, Schulze, & Mooney, 1990; Kobe, 1997; O'Brien, Leuzinger, Philipson, Tay, & Hector, 2014), and seasonally to construct new tissues (Barbaroux & Bréda, 2002). There is widespread interest in the complexities underlying NSC storage and use (Palacio, Hoch, Sala, Körner, & Millard, 2014), and NSC dynamics likely play a role in the high correlation of ring-width series with previous growing season climate (Dietze et al., 2014).

Longer lags (e.g. 2 to 4+ years) are more difficult to explain, but may be driven by one or more of a combination of physiological factors such as (1) hydraulic constraints, (2) legacy effects of past needle cohorts or wood features or (3) NSC storage dynamics. First, multi-year persistence of hydraulic limitations (unrepaired embolism) leading to decreased growth has been suggested as a mechanism underlying legacy effects of drought in conifers in the Southwest (Anderegg et al., 2015; Peltier et al., 2016). Similar effects could arise due to sapwood depth reduction caused by water stress (Cermak & Nadezhdina, 1998; Phillips, Oren, & Zimmermann, 1996). While the magnitude of older weights was usually small relative to weights defining the importance of more recent climate conditions (Figure 4), the frequency of high drought stress is likely to increase in this region (Seager et al., 2007), potentially increasing the importance of drought legacy effects on tree growth and forest productivity (Schwalm et al., 2017). Second, each of the conifer species studied here can retain needles for at least two, or as many as 7 years (Little, 1980). Poor needle crops in a given year could thus effect growth rates for many subsequent years. Third, the long lags present in PDSI effects for *P. edulis*, *P. ponderosa* and *P. menziesii* and in temperature effects for *P. edulis* could also indicate long-term differences in NSC storage between trees or sites. This may be due to use of multiple NSC pools of differing ages and turnover times (Carbone et al., 2013; Muhr et al., 2016; Richardson et al., 2015; Trumbore, Czimczik, Sierra, Muhr, & Xu, 2015), or trees entering different "states" associated with either favourable or poor growing conditions (Ogle & Pacala, 2009). Experimental work, however, is required to identify the actual mechanisms underlying predicted lagged effects of climate on tree growth.

4.4 | Spatial variation in climatic sensitivities and NAM

Variations in the sensitivities of ring-width indices to antecedent climate variables across the Southwest suggest important differences in tree physiology within a species' range associated with climate regime, elevation and/or genetic variation (Table 1). Latitudinal variations in tree-ring growth sensitivities are well-documented, as trees shift from precipitation to temperature limitation with increases in latitude and/or elevation (Douglass, 1937). Different *P. ponderosa* subspecies occupy the north and south of the Southwest region (Willyard et al., 2017), which may underlie lower baseline growth (RWI_c^*) and autoregressive terms for this species at higher latitudes (Table 1). Differential moisture use and summer precipitation variability along the latitudinal gradient of relative precipitation contribution of the NAM may also drive these responses (Szejner et al., 2016).

Climatic differences, such as the relative contribution of Pacific winter storms vs. the NAM to annual precipitation, may also underlie east to west variation in baseline growth rates, autocorrelation, and PDSI sensitivity in *P. edulis*, *P. ponderosa* and *P. menziesii* (Table 1). Sites farther west generally experience the bimodal precipitation regime characteristic of Arizona—relatively equal precipitation inputs during winter and the summer monsoon with a pronounced dry period in March-June—whereas sites further east receive a smaller proportion of precipitation during the winter (Douglas, Maddox, Howard, & Reyes, 1993; Griffin et al., 2013; Higgins, Yao, & Wang, 1997; Szejner et al., 2016). Tree rings in the Southwest can be highly sensitive to the timing, duration and magnitude of monsoonal precipitation. For example, sub-annual characteristics of tree rings from trees in the Southwest, such as occurrence and location of false latewood bands, are highly sensitive to onset date and strength of the NAM, and these sensitivities differ between sites (Babst et al., 2016). North American Monsoon characteristics are also strong drivers of latewood $\delta^{13}C$—an integrated physiological measure of water-use efficiency—in this region (Leavitt, Wright, & Long, 2002). For example, monsoon arrival "rescues" trees from mid-summer drought; in more arid western sites higher sensitivity to positive PDSI and a more negative sensitivity to temperature (*P. edulis*) may be due to more variable monsoon arrival and intensity (Figure 3). As winter and early spring precipitation are the most consistently important drivers of ring widths in *P. ponderosa*, *P. edulis* and *P. menziesii*, we find lower average growth rates in the more eastern sites (Figure 3; Fritts et al., 1965). Highly variable NAM onset date may also underlie weaker autoregressive effects and lower baseline growth in eastern sites, which derive less of their annual precipitation from winter storms (see above; Table 1). However, this could also be due to greater dependence on stored NSCs for growth in more arid sites, reflecting a link between stress and physiological strategy at the population or genotype level (Chen et al., 2010; Grady et al., 2013).

5 | CONCLUSIONS AND FUTURE WORK

Our application of the SAM framework demonstrates the importance of considering antecedent climate, even in detrended annual ring-width series, and how growth in closely related species can depend to varying degrees on different antecedent climate variables. We argue that the SAM approach represents a rigorous method for selecting antecedent climate variables for use in tree–growth–climate modelling applications, because it allows data and models to inform the selection process. In the future, we hope to explicitly include spatial effects (e.g. elevation, latitude, etc.) into the SAM model to understand how, in addition to sensitivities to various climate variables, the antecedent weights themselves vary through time and space. While we would like to incorporate more species to understand how the effects of antecedent climate differ across less related groups of species (e.g. angiosperms vs. gymnosperms). Sample size for other species was insufficient, highlighting the need for better replication of unconventional dendrochronology species if data synthesis studies are to be representative of the range of growth and physiological strategies in North America. Moreover, results from our application of the SAM model provide evidence that regional climate may drive differences in climatic sensitivities within a species' range, suggesting regional vegetation models should account for variation across populations, particularly in the context of climate change, where different populations may differentially respond to such changes (Chen et al., 2010).

ACKNOWLEDGEMENTS

This work was funded by a National Science Foundation Advances in Biological Informatics award (DBI#1458867). We thank William Cable for obtaining tree-ring data from the ITRDB, Joshua Uebelherr for downloading and preparing the CRU dataset, Ryan Bishop for help collating dendrochronology articles, and the Ogle Laboratory for comments on earlier versions.

AUTHORS' CONTRIBUTIONS

D.M.P.P., J.J.B. and K.O. conceived the statistical model; D.M.P.P. and K.O. conducted the analysis; D.M.P.P. led the writing of the manuscript. All authors contributed critically to the drafts and gave final approval for publication.

DATA ACCESSIBILITY

Model code is archived on Github: https://github.com/drewpeltier/Stochastic-Antecedent-Model---Dendrochronologies (Peltier, 2017). Dendrochronology data are freely available on the International Tree Ring Data Bank https://www.ncdc.noaa.gov/data-access/paleoclimatology-data/datasets/tree-ring. The names of all dendrochronologies we used are noted in Table S1. Climate data are freely available from the Climatic Research Unit (CRU TS3.10): http://catalogue.ceda.ac.uk/uuid/3f8944800cc48e1cbc29a5ee12d8542d. Dai Palmer Drought Severity Index data provided by the NOAA/OAR/ESRL PSD, Boulder, Colorado, USA, from their Web site at http://www.esrl.noaa.gov/psd.

ORCID

Drew M. P. Peltier http://orcid.org/0000-0003-3271-9055

REFERENCES

Adams, H. D., & Kolb, T. E. (2005). Tree growth response to drought and temperature in a mountain landscape in northern Arizona, USA. *Journal of Biogeography*, *32*, 1629–1640.

Anderegg, W. R. L., Schwalm, C., Biondi, F., Camarero, J. J., Koch, G., Litvak, M., … Pacala, S. (2015). Pervasive drought legacies in forest ecosystems and their implications for carbon cycle models. *Science*, *349*, 528–532.

Babst, F., Wright, W. E., Szejner, P., Wells, L., Belmecheri, S., & Monson, R. K. (2016). Blue intensity parameters derived from Ponderosa pine tree rings characterize intra-annual density fluctuations and reveal seasonally divergent water limitations. *Trees*, *30*, 1403–1415.

Barbaroux, C., & Bréda, N. (2002). Contrasting distribution and seasonal dynamics of carbohydrate reserves in stem wood of adult ring-porous sessile oak and diffuse-porous beech trees. *Tree Physiology*, *22*, 1201–1210.

Barger, N. N., & Woodhouse, C. (2015). Piñon pine (*Pinus edulis* Engelm.) growth responses to climate and substrate in southern Utah, USA. *Plant Ecology*, *216*, 913–923.

Barron-Gafford, G. A., Cable, J. M., Bentley, L. P., Scott, R. L., Huxman, T. E., Jenerette, G. D., & Ogle, K. (2014). Quantifying the timescales over which exogenous and endogenous conditions affect soil respiration. *New Phytologist*, *202*, 442–454.

Becker, M. (1989). The role of climate on present and past vitality of silver fir forests in the Vosges mountains of northeastern France. *Canadian Journal of Forest Research*, *19*, 1110–1117.

Bigler, C., Gavin, D. G., Gunning, C., & Veblen, T. T. (2007). Drought induces lagged tree mortality in a subalpine forest in the Rocky Mountains. *Oikos*, *116*, 1983–1994.

Blasing, T. J., Solomon, A. M., & Duvick, D. N. (1986). Response functions revisited. *Tree-Ring Bulletin*, *44*, 1–15.

Bond-Lamberty, B., Rocha, A. V., Calvin, K., Holmes, B., Wang, C., & Goulden, M. L. (2014). Disturbance legacies and climate jointly drive tree growth and mortality in an intensively studied boreal forest. *Global Change Biology*, *20*, 216–227.

Bunn, A. G. (2008). A dendrochronology program library in R (dplR). *Dendrochronologia*, *26*, 115–124.

Cable, J. M., Ogle, K., Barron-Gafford, G. A., Bentley, L. P., Cable, W. L., Scott, R. L., … Huxman, T. E. (2013). Antecedent conditions influence soil respiration differences in shrub and grass patches. *Ecosystems*, *16*, 1230–1247.

Campelo, F., Nabais, C., Garcia-Gonzalez, I., Cherubini, P., Gutierrez, E., & Freitas, H. (2009). Dendrochronology of *Quercus ilex* L. and its potential use for climate reconstruction in the Mediterranean region. *Canadian Journal of Forest Research*, *39*, 2486–2493.

Carbone, M. S., Czimczik, C. I., Keenan, T. F., Murakami, P. F., Pederson, N., Schaberg, P. G., … Richardson, A. D. (2013). Age, allocation and availability of nonstructural carbon in mature red maple trees. *New Phytologist*, *200*, 1145–1155.

Carrer, M., Motta, R., & Nola, P. (2012). Significant mean and extreme climate sensitivity of Norway spruce and silver fir at mid-elevation mesic sites in the Alps. *PLoS ONE*, *7*, e50755.

Carrer, M., & Urbinati, C. (2006). Long-term change in the sensitivity of tree-ring growth to climate forcing in *Larix decidua*. *New Phytologist*, *170*, 861–872.

Cermak, J., & Nadezhdina, N. (1998). Sapwood as the scaling parameter-defining according to xylem water content or radial pattern of sap flow? *Annales Des Sciences Forestieres*, *55*, 509–521.

Chapin, F. S. III, Schulze, E. D., & Mooney, H. A. (1990). The ecology and economics of storage in plants. *Annual Review of Ecology and Systematics*, *21*, 423–447.

Chen, P.-Y., Welsh, C., & Hamann, A. (2010). Geographic variation in growth response of Douglas-fir to interannual climate variability and projected climate change. *Global Change Biology*, *16*, 3374–3385.

Cook, E. R., & Peters, K. (1981). The smoothing spline: A new approach to standardizing forest interior tree-ring width series for dendroclimatic studies. *Tree-Ring Bulletin*, *41*, 45–53.

Copenheaver, C. A., Kyle, K. H., Stevens, G. N., & Kamp, M. H. (2005). Comparing *Juniperus virginiana* tree-ring chronologies from forest edge vs. forest interior positions in the Cedars Natural Area Preserve in Virginia, USA. *Dendrochronologia*, *23*, 39–45.

Dai, A., Trenberth, K. E., & Qian, T. (2004). A global dataset of Palmer Drought Severity Index for 1870-2002: Relationship with soil moisture and effects of surface warming. *Journal of Hydrometeorology*, *5*, 1117–1130.

Dal Bello, M., Rindi, L., & Benedetti-Cecchi, L. (2017). Legacy effects and memory loss: How contingencies moderate the response of rocky intertidal biofilms to present and past extreme events. *Global Change Biology*, *23*, 3259–3268.

Di Filippo, A., Biondi, F., Čufar, K., De Luis, M., Grabner, M., Maugeri, M., … Piovesan, G. (2007). Bioclimatology of beech (*Fagus sylvatica* L.) in the Eastern Alps: Spatial and altitudinal climatic signals identified through a tree-ring network. *Journal of Biogeography*, *34*, 1873–1892.

Dietze, M. C., Sala, A., Carbone, M. S., Czimczik, C. I., Mantooth, J. A., Richardson, A. D., & Vargas, R. (2014). Nonstructural carbon in woody plants. *Annual Review of Plant Biology*, *65*, 667–687.

Douglas, M. W., Maddox, R. A., Howard, K., & Reyes, S. (1993). The Mexican monsoon. *Journal of Climate*, *6*, 1665–1677.

Douglass, A. E. (1937). Tree-ring work, 1937. *Tree-Ring Bulletin*, *4*, 3–6.

Fritts, H. C. (1962). An approach to dendroclimatology: Screening by means of multiple regression techniques. *Journal of Geophysical Research*, *67*, 1413–1420.

Fritts, H. (1966). Growth-rings of trees: Their correlation with climate. *Science*, *154*, 974–979.

Fritts, H. C. (1976). *Tree rings and climate* (p. 567). San Diego, CA: Academic Press.

Fritts, H. C., Smith, D. G., Cardis, J. W., & Budelsky, C. A. (1965). Tree-ring characteristics along a vegetation gradient in northern Arizona. *Ecology*, *46*, 394–401.

Fritts, H. C., & Swetnam, T. W. (1989). Dendroecology: A tool for evaluating. *Advances in Ecological Research*, *19*, 111–188.

Grace, J., & Norton, D. (1990). Climate and growth of *Pinus-sylvestris* at its upper altitudinal limit in Scotland – Evidence from tree growth-rings. *Journal of Ecology*, *78*, 601–610.

Grady, K. C., Laughlin, D. C., Ferrier, S. M., Kolb, T. E., Hart, S. C., Allan, G. J., & Whitham, T. G. (2013). Conservative leaf economic traits correlate with fast growth of genotypes of a foundation riparian species near the thermal maximum extent of its geographic range. *Functional Ecology*, *27*, 428–438.

Griffin, D., Woodhouse, C. A., Meko, D. M., Stahle, D. W., Faulstich, H. L., Carrillo, C., … Leavitt, S. W. (2013). North American monsoon precipitation reconstructed from tree-ring latewood. *Geophysical Research Letters*, *40*, 954–958.

Harris, I., Jones, P. D., Osborn, T. J., & Lister, D. H. (2014). Updated high-resolution grids of monthly climatic observations – The CRU TS3.10 Dataset. *International Journal of Climatology*, *34*, 623–642.

Higgins, R. W., Yao, Y., & Wang, X. L. (1997). Influence of the North American monsoon system on the US summer precipitation regime. *Journal of Climate*, *10*, 2600–2622.

Jenkins, M. A., & Pallardy, S. G. (1995). The influence of drought on red oak group species growth and mortality in the Missouri Ozarks. *Canadian Journal of Forest Research*, *25*, 1119–1127.

Johnson, F., & Risser, P. (1973). Correlation analysis of rainfall and annual ring index of central Oklahoma blackjack and post oak. *American Journal of Botany*, *60*, 475–478.

Keen, F. P. (1937). Climatic cycles in eastern Oregon as indicated by tree rings. *Monthly Weather Review*, *65*, 175–188.

Kirdyanov, A. V., Vaganov, E. A., & Hughes, M. K. (2007). Separating the climatic signal from tree-ring width and maximum latewood density records. *Trees-Structure and Function*, *21*, 37–44.

Kobe, R. K. (1997). Carbohydrate allocation to storage as a basis of interspecific variation in sapling survivorship and growth. *Oikos*, *80*, 226–233.

Leavitt, S. W., Wright, W. E., & Long, A. (2002). Spatial expression of ENSO, drought, and summer monsoon in seasonal δ13C of ponderosa pine

tree rings in southern Arizona and New Mexico. *Journal of Geophysical Research: Atmospheres*, *107*, 4349.

Little, E. L. (1980). *The Audubon Society field guide to North American trees*. New York, NY: Alfred A. Knopf.

Mäkinen, H., Nöjd, P., Kahle, H.-P., Neumann, U., Tveite, B., Mielikäinen, K., … Spiecker, H. (2002). Radial growth variation of Norway spruce (*Picea abies* (L.) Karst.) across latitudinal and altitudinal gradients in central and northern Europe. *Forest Ecology and Management*, *171*, 243–259.

Mazza, G., & Manetti, M. C. (2013). Growth rate and climate responses of *Pinus pinea* L. in Italian coastal stands over the last century. *Climatic Change*, *121*, 713–725.

Michelot, A., Simard, S., Rathgeber, C., Dufrêne, E., & Damesin, C. (2012). Comparing the intra-annual wood formation of three European species (*Fagus sylvatica*, *Quercus petraea* and *Pinus sylvestris*) as related to leaf phenology and non-structural carbohydrate dynamics. *Tree Physiology*, *32*, 1033–1045.

Muhr, J., Messier, C., Delagrange, S., Trumbore, S., Xu, X., & Hartmann, H. (2016). How fresh is maple syrup? Sugar maple trees mobilize carbon stored several years previously during early springtime sap-ascent. *New Phytologist*, *209*, 1410–1416.

Nehrbass-Ahles, C., Babst, F., Klesse, S., Nötzli, M., Bouriaud, O., Neukom, R., … Frank, D. (2014). The influence of sampling design on tree-ring-based quantification of forest growth. *Global Change Biology*, *20*, 2867–2885.

O'Brien, M. J., Leuzinger, S., Philipson, C. D., Tay, J., & Hector, A. (2014). Drought survival of tropical tree seedlings enhanced by non-structural carbohydrate levels. *Nature Climate Change*, *4*, 710–714.

Ogle, K., & Barber, J. J. (2016). Plant and ecosystem memory. *Chance*, *29*, 16–22.

Ogle, K., Barber, J. J., Barron-Gafford, G. A., Bentley, L. P., Cable, J. M., Huxman, T. E., … Tissue, D. T. (2015). Quantifying ecological memory in plant and ecosystem processes. *Ecology Letters*, *18*, 221–235.

Ogle, K., & Pacala, S. W. (2009). A modeling framework for inferring tree growth and allocation from physiological, morphological and allometric traits. *Tree Physiology*, *29*, 587–605.

Palacio, S., Hoch, G., Sala, A., Körner, C., & Millard, P. (2014). Does carbon storage limit tree growth? *New Phytologist*, *201*, 1096–1100.

Peltier, D. M. P. (2017). Data from: Quantifying antecedent climatic drivers of tree growth in the Southwestern US. Github. https://github.com/drewpeltier/Stochastic-Antecedent-Model---Dendrochronologies

Peltier, D. M. P., Fell, M., & Ogle, K. (2016). Legacy effects of drought in the southwestern United States: A multi-species synthesis. *Ecological Monographs*, *86*, 312–326.

Phillips, N., Oren, R., & Zimmermann, R. (1996). Radial patterns of xylem sap flow in non-, diffuse-and ring-porous tree species. *Plant, Cell & Environment*, *19*, 983–990.

Plummer, M. (2003). JAGS: A program for analysis of Bayesian graphical models using Gibbs sampling. Proceedings of the 3rd international workshop on distributed statistical computing, p. 125. Vienna, Austria. Retrieved from https://www.r-project.org/conferences/DSC-2003/Proceedings/Plummer.pdf

Plummer, M. (2013). Rjags: Bayesian graphical models using MCMC. R Package Version 3–10. Retrieved from http://CRAN.R-project.org/package=rjags

R Core Team. (2016). *R: A language and environment for statistical computing*. Vienna, Austria: R Foundation for Statistical Computing.

Richardson, A. D., Carbone, M. S., Huggett, B. A., Furze, M. E., Czimczik, C. I., Walker, J. C., … Murakami, P. (2015). Distribution and mixing of old and new nonstructural carbon in two temperate trees. *New Phytologist*, *206*, 590–597.

Ryan, E. M., Ogle, K., Peltier, D., Walker, A. P., De Kauwe, M. G., Medlyn, B. E., … Pendall, E. (2017). Gross primary production responses to warming, elevated CO_2, and irrigation: Quantifying the drivers of ecosystem physiology in a semiarid grassland. *Global Change Biology*, *23*, 3092–3106.

Ryan, E. M., Ogle, K., Zelikova, T. J., LeCain, D. R., Williams, D. G., Morgan, J. A., & Pendall, E. (2015). Antecedent moisture and temperature conditions modulate the response of ecosystem respiration to elevated CO_2 and warming. *Global Change Biology*, *21*, 2588–2602.

Sarris, D., Christodoulakis, D., & Koerner, C. (2007). Recent decline in precipitation and tree growth in the eastern Mediterranean. *Global Change Biology*, *13*, 1187–1200.

Schwalm, C., Anderegg, W. R. L., Michalak, A. M., Fisher, J. B., Biondi, F., Koch, G., … Tian, H. (2017). Global patterns of drought recovery. *Nature*, *548*, 202–205.

Seager, R., Ting, M., Held, I., Kushnir, Y., Lu, J., Vecchi, G., … Naik, N. (2007). Model projections of an imminent transition to a more arid climate in southwestern North America. *Science*, *316*, 1181–1184.

Stahle, D. W., Cleaveland, M. K., & Hehr, J. G. (1985). A 450-year drought reconstruction for Arkansas, United States. *Nature*, *316*, 530–532.

Szejner, P., Wright, W. E., Babst, F., Belmecheri, S., Trouet, V., Leavitt, S. W., … Monson, R. K. (2016). Latitudinal gradients in tree-ring stable carbon and oxygen isotopes reveal differential climate influences of the North American monsoon system. *Journal of Geophysical Research: Biogeosciences*, *121*, 1978–1991.

Tainter, F. H., Retzlaff, W. A., Starkey, D. A., & Oak, S. W. (1990). Decline of radial growth in red oaks is associated with short-term changes in climate. *European Journal of Forest Pathology*, *20*, 95–105.

Tingley, M. P., Craigmile, P. F., Haran, M., Li, B., Mannshardt, E., & Rajaratnam, B. (2012). Piecing together the past: Statistical insights into paleoclimatic reconstructions. *Quaternary Science Reviews*, *35*, 1–22.

Trumbore, S., Czimczik, C. I., Sierra, C. A., Muhr, J., & Xu, X. (2015). Nonstructural carbon dynamics and allocation relate to growth rate and leaf habit in California oaks. *Tree Physiology*, *35*, 1206–1222.

Veblen, T. T., Kitzberger, T., & Donnegan, J. (2000). Climatic and human influences on fire regimes in ponderosa pine forests in the Colorado Front Range. *Ecological Applications*, *10*, 1178–1195.

Villalba, R., Veblen, T. T., & Ogden, J. (1994). Climatic influences on the growth of sub-alpine trees in the Colorado Front Range. *Ecology*, *75*, 1450–1462.

Weaver, H. (1943). Fire as an ecological and silvicultural factor in the ponderosa-pine region of the pacific slope. *Journal of Forestry*, *41*, 7–15.

Willyard, A., Gernandt, D. S., Potter, K., Hipkins, V., Marquardt, P., Mahalovich, M. F., … Wofford, A. (2017). *Pinus ponderosa*: A checkered past obscured four species. *American Journal of Botany*, *104*, 161–181.

Wilmking, M., Juday, G. P., Barber, V. A., & Zald, H. S. J. (2004). Recent climate warming forces contrasting growth responses of white spruce at treeline in Alaska through temperature thresholds. *Global Change Biology*, *10*, 1724–1736.

SUPPORTING INFORMATION

Additional Supporting Information may be found online in the supporting information tab for this article.

How to cite this article: Peltier DMP, Barber JJ, Ogle K. Quantifying antecedent climatic drivers of tree growth in the Southwestern US. *J Ecol*. 2017;00:1–12. https://doi.org/10.1111/1365-2745.12878